

## Determination of Microscopic Equilibrium Constants for the Complexation of Ditopic Guests by Cyclodextrins from NMR Experiments

A. Jover,<sup>†</sup> Rosane M. Budal,<sup>‡</sup> F. Meijide,<sup>†</sup> Victor Hugo Soto,<sup>†</sup> and J. Vázquez Tato<sup>\*,†</sup>

*Departamento de Química Física, Facultad de Ciencias, Universidad de Santiago de Compostela, Campus de Lugo, Spain, and Departamentos de Química y Ciencias Farmacéuticas, Universidade Federal de Santa Catarina, Florianópolis, SC, Brasil*

*Received: October 10, 2003; In Final Form: September 20, 2004*

The complexation of 3-[(3-cholamidopropyl)dimethylammonio]-1-propanesulfonate (CHAPS) by  $\beta$ - and  $\gamma$ -cyclodextrin ( $\beta$ - and  $\gamma$ -CD) has been studied by using 1D- and 2D-NMR techniques. For the CHAPS/ $\beta$ -CD system both  $^{13}\text{C}$  and  $^1\text{H}$  NMR spectra exhibit split lines consistent with slow exchange rate between one or more complexes and free species. Job's plots suggest that complexes with 1:1 stoichiometry are formed. However, ROESY experiments suggest that  $\beta$ -CD is complexing the steroid nucleus at two sites, the first one being mainly the side chain of the guest, and the second one being the A/B rings. The conclusion is that two isomeric 1:1 complexes,  $C_{11}^Y$  and  $C_{11}^X$ , are obtained. The concentrations of free and complexed species were measured from the integration of  $^1\text{H}$  NMR signals, allowing an independent determination of the two microscopic equilibrium constants,  $K_{11}^Y$  and  $K_{11}^X$ , associated with the formation of the two isomeric complexes, and the macroscopic equilibrium constant,  $K_{11}$  ( $= K_{11}^X + K_{11}^Y$ ). A good agreement between the values obtained is observed. The slow exchange rate for the formation and decomposition of the  $C_{11}^Y$  complex is understood as a barrier penetration problem for the side chain to cross through the cyclodextrin cavity since the methyl groups linked to the charged nitrogen atom of the side chain are bulky enough to force a large distortion of the  $\beta$ -CD during the penetration. However, the origin of the energy barrier for the complexation of the wide end of the steroid nucleus leading to a slow exchange regime is unknown. The travelling of the CHAPS side chain through a larger cyclodextrin cavity should be faster. Therefore, complexation studies between CHAPS and  $\gamma$ -CD were undertaken. Now, only one type of complex was observed and the fast limited exchange was obeyed. The value for the equilibrium formation constant was obtained from the analysis of the chemical shift displacements of carbon atoms of  $\gamma$ -CD with increasing CHAPS concentration. ROESY experiments suggest that the side chain is unfolded outside the cyclodextrin cavity forming a rotaxane-type structure.

### Introduction

The determination of microscopic equilibrium constants is a problem present in all systems with multiple binding sites. Examples are the acid–base equilibria of amino acids, the interaction between macromolecules (including DNA, protein, etc.) and ligand (including drugs, ions, surfactants, etc.),<sup>1–3</sup> activation of ion channels,<sup>4</sup> ligand–receptor<sup>5</sup> and ligand–enzyme<sup>6</sup> interactions,<sup>7</sup>  $\text{Na}^+/\text{K}^+$ -transport and ATP–enzyme interactions,<sup>8–10</sup> etc. Unfortunately, the determination of microscopic constants is not always experimentally accessible and only macroscopic constants (which are relationships between the microscopic ones) can be obtained. Extra-thermodynamic assumptions (models concerning independent or identical sites, use of values taken from similar systems, etc.) are usually accepted for solving the problem.

Only a few determinations of microscopic binding constants in cyclodextrin systems can be found in the literature. (Natural cyclodextrins are cyclic oligomers built up from 6, 7, or 8 glucopyranose units (named  $\alpha$ -,  $\beta$ -, and  $\gamma$ -CD, respectively) linked by  $\alpha$ -(1–4)-glycosidic bonds.<sup>30</sup> They have been used as

enzyme models and artificial enzymes<sup>34–37</sup> and have many practical applications in pharmacy and engineering.<sup>30</sup>) Connors et al. have studied the complexation of sym-1,4-disubstituted benzenes<sup>11</sup> and sym-4,4'-disubstituted biphenyls,<sup>12</sup> while Sur and Bryant<sup>13</sup> have studied the complexation of some porphyrins. For these symmetrical guests, the relationships between microscopic and macroscopic binding constants are greatly simplified, allowing the determination of the microscopic binding constants.<sup>11</sup> This determination has been possible for some non-symmetrical guests,<sup>14</sup> but the equilibrium constant values were approximate and previous knowledge of the values of macroscopic constants was required.

NMR spectroscopies are the most promising techniques for measuring microscopic equilibrium constants as they give direct information about the electronic environment of a specific nucleus. Examples of this application in acid–base equilibria can be found in the literature.<sup>15</sup>

Two exchange rate limits can be found in NMR spectroscopy.<sup>16</sup> When the host–guest complexation equilibrium has a very fast exchange rate compared to the NMR time scale, the chemical shift of a nucleus observed in a host–guest mixture is the mole fraction weighted average of the chemical shifts of the free and complexed molecules.<sup>17</sup> The analysis of the chemical shift displacements (usually obtained from  $^1\text{H}$  and  $^{13}\text{C}$

\* Corresponding author.

<sup>†</sup> Universidad de Santiago de Compostela.

<sup>‡</sup> Universidade Federal de Santa Catarina.

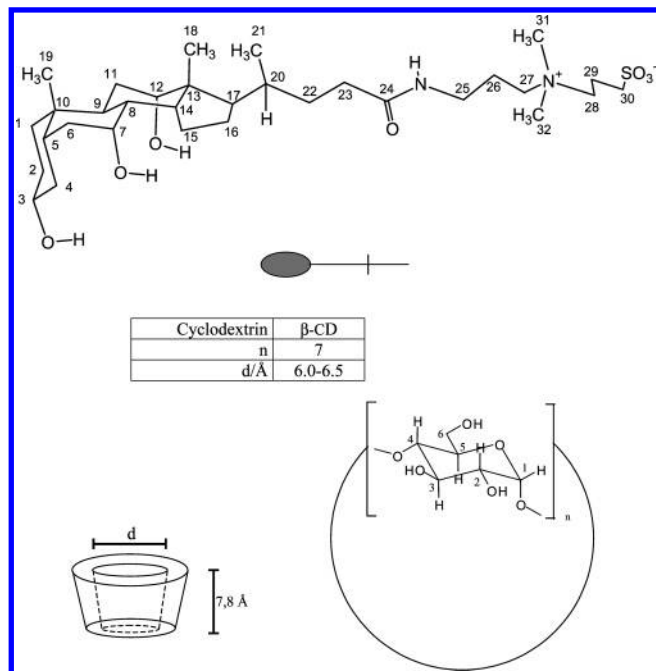


**Figure 1.** Schematic structures of CHAPS and  $\beta$ -cyclodextrin.

NMR experiments) in mixtures of different [guest]/[host] ratios,<sup>18</sup> allows the determination of the equilibrium constants for the formation of the inclusion compounds. This methodology was used to determine the equilibrium constants for bile salt/cyclodextrin systems.<sup>19</sup> [The interaction between cyclodextrins and steroids (mainly hormones,<sup>38,39</sup> cholesterol<sup>40–47</sup> and bile salts<sup>19,48</sup>) is a subject of an increasing interest.<sup>18,19,49</sup> It has been shown that trihydroxy bile salts behave as monotopic guests with  $\beta$ -CD (forming complexes with a 1:1 stoichiometry), while dihydroxy bile salts are ditopic guests forming 1:2 complexes.<sup>19,22</sup> Furthermore, the behavior of ditopic guests (as dihydroxy bile salts) with ditopic hosts (i.e., cyclodextrin dimers) is an important subject in cyclodextrin supramolecular chemistry since they can give rise to either the chelate binding effect<sup>36,50–57</sup> or to the formation of supramolecular conglomerates (oligomers or polymers).<sup>19,49,58,59</sup>] On the other hand, when the host–guest complexation equilibrium has a slow exchange rate compared to the NMR time scale, the signals of the host and guest nuclei in the complex and free species appear at different chemical shifts. Cameron et al.<sup>20</sup> have observed an example of a slow exchange rate on the NMR time scale when studying the complexation of a steroidal neuromuscular blocker drug by Org25969 (a  $\gamma$ -CD derivative).

This slow exchange regime is quite favorable for the determination of microscopic constants but, to our knowledge, it has not been employed for measuring microscopic equilibrium constants in cyclodextrin systems. In the example presented here (CHAPS, Figure 1, a derivative of sodium cholate, was chosen as guest) no models concerning independent or identical sites have been used and the involved macroscopic and microscopic equilibrium constants were obtained from independent measurements. The binding of steroids to cyclodextrins has been used as a model for steroid–protein interactions,<sup>21</sup> and therefore the present methodology can be useful in solving more complex biological systems.

## Experimental Section

CHAPS (ICN Biomedicals Inc.) was used without further purification.  $\beta$ -CD (kindly supplied by Roquette, France) and

$\gamma$ -CD (Wacker, Germany) were recrystallized twice from distilled water and dried in a vacuum oven. D<sub>2</sub>O (99.90%) was supplied by SDS (France). When necessary, acidity was adjusted with KOD (Aldrich, 40% in D<sub>2</sub>O) to final pD values in the range 7–8.

Stock solutions of CHAPS and cyclodextrins were prepared with D<sub>2</sub>O as solvent. Samples were prepared directly in the NMR tubes. Spectra were recorded using a Bruker AMX-500 NMR spectrometer operating at 500 MHz for <sup>1</sup>H and 125 MHz for <sup>13</sup>C. TMS was used as external reference.<sup>13</sup>C experiments were recorded on a Bruker AC-300 NMR spectrometer operating at 75 MHz and 293.1 K.

Conditions for ROESY were as follows: relaxation delay, 0 s; mixing time, 300 ms; spectral width, 10 ppm with 1024 complex points in *f*<sub>2</sub>; 128 *t*<sub>1</sub> values and 8 scans per *t*<sub>1</sub> value; *T* = 298.1 K.

## Results and Discussion

Figure 2a shows the <sup>13</sup>C NMR spectra of the CHAPS/ $\beta$ -CD system at different [CHAPS]/[ $\beta$ -CD] ratios, the sum of concentration of guest (CHAPS) and host ( $\beta$ -CD) being constant and equal to 10 mM. This is a typical set of experiments carried out to determine the stoichiometry of the inclusion complex from Job's plot.<sup>22</sup> For most bile salt/ $\beta$ -CD systems,<sup>18,19,22</sup> an induced change in the chemical shifts of carbon atoms of  $\beta$ -CD with increasing the [guest]/[host] ratio can be observed, resulting from the condition of fast exchange rate.

<sup>13</sup>C (for CHAPS and  $\beta$ -CD) chemical shifts do not move as a function of [ $\beta$ -CD]/[CHAPS] as can be noticed in Figures 2a and 2b for  $\beta$ -CD and CHAPS, respectively. In Figure 2b it must be noticed that carbon atoms belong to any of the four cycles and side chain of CHAPS. Under fast exchange conditions a move of these signals with varying concentration (i.e., with the [CHAPS]/[ $\beta$ -CD] ratio) should be detected. However, the signals of the C1–C5 carbon atoms of  $\beta$ -CD are split, the split being independent of the [CHAPS]/[ $\beta$ -CD] ratio, while C6 appears as an unchanged single signal. The split is better observed for C1 and C4 carbon atoms (Figure 2a) and is less evident for C2 and C5. Emergent split peaks can be observed with a simultaneous decrease of the intensities of free  $\beta$ -CD signals when [CHAPS]/[ $\beta$ -CD] ratio rises (see the lower spectrum of Figure 2b). For the lower concentrations of CHAPS, the signals due to carbon atoms of CHAPS are not detected, even with long accumulation times. These facts suggest that the complexation equilibrium has a slow exchange rate—NMR time scale.<sup>16</sup> The split of peaks is not due to the formation of CHAPS micelles since no changes of this magnitude are observed in its pure NMR spectra even at the maximum concentration employed in the complexation studies (cmc values in the range 4–14 mM have been published for CHAPS).<sup>23–26</sup>

The slow exchange rate condition was also observed in <sup>1</sup>H NMR spectra (Figure 3) since the signals corresponding to the hydrogen atoms P12, P18, P19, P21, P25 and P30 are split. (In what follows, P and H represent protons of the steroid and cyclodextrin, respectively, and the number indicates the carbon atom to which the hydrogen atom is bound.) This is also the case of P6 and P5 (not shown in the Figure). These comments are also valid for H3, H5, and H6, although H5-free is masked by signals at  $\delta$  3.74–3.66 ppm. H1 and H4 remain unchanged and there is a slight change in the chemical shift of H2. [It seems that some chemical shifts (mainly those of P6, P12, P18, and P19, free or complexed) move as a function of concentration

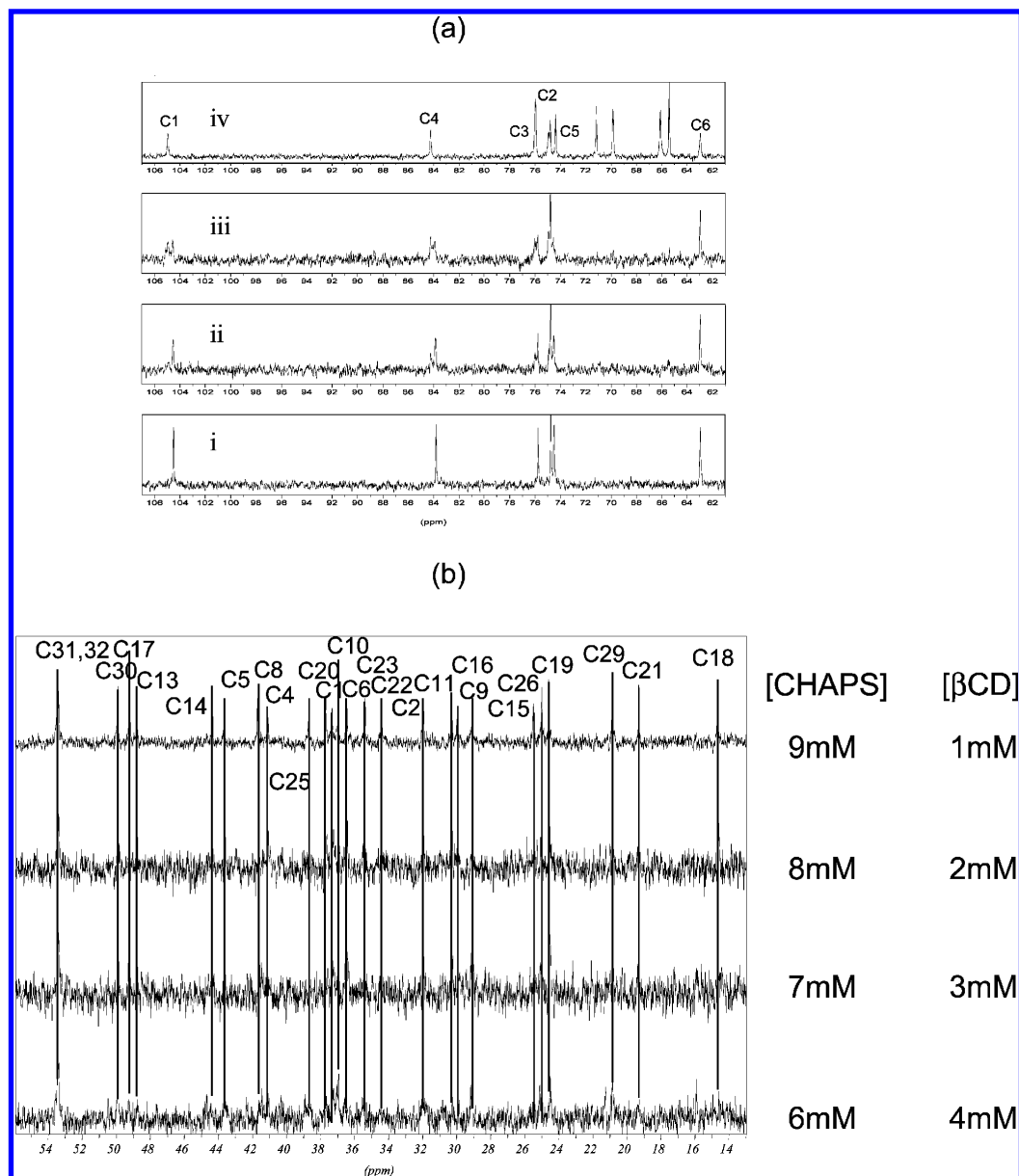


**Figure 2.** (a)  $^{13}\text{C}$  NMR spectra of the CHAPS/ $\beta$ -CD/ $\text{D}_2\text{O}$  system at the following concentrations: (i)  $\beta$ -CD 10 mM, CHAPS 0 mM; (ii)  $\beta$ -CD 7 mM, CHAPS 3 mM; (iii)  $\beta$ -CD 5 mM, CHAPS 5 mM; and (iv)  $\beta$ -CD 1 mM, CHAPS 9 mM. (b) Constancy of the  $^{13}\text{C}$  chemical shifts for CHAPS and  $\beta$ -CD. In the lower spectrum some split signals are emerging from the noise level.

of CHAPS, the maximum movements corresponding to P19 (free), 0.028 ppm, and P6 (complex), 0.030 ppm. However, it is necessary to take into account the experimental error. The minimum error in chemical shifts for a given proton in a set of repeated experiments is  $\sigma_{\Delta\delta} = \pm 5 \times 10^{-3}$  ppm, although usually it is higher. Only a few experimental values of the moving signals are outside the range of that minimum error and therefore, within experimental error, the movement of chemical shifts as a function of concentration of CHAPS is negligible. Furthermore, the direction of the shifts for the free signals is opposite to that observed for bile salts.<sup>22</sup> It can be concluded that all of these small shifts may be just due to effects of different concentrations of compounds on the nature (polarity or bulk magnetic susceptibility) of the medium.]

González Gaitano et al.<sup>27</sup> and Ramos Cabrer<sup>28</sup> have published  $\Delta\delta_{\text{max}} = \delta_{\text{complex}} - \delta_{\text{free}}$  values for some protons for the  $\beta$ -CD/sodium cholate system (which obeys fast exchange on the NMR time scale), the values being 0.12–0.14 (P18 and P21) and 0.07 (P19). The measured  $\Delta\delta_{\text{max}}$  values between the splitting into

pair (free and complex) signals for the same protons are 0.15 (P18 and P21) and 0.05 (P19). This remarkable agreement strongly supports the slow exchange regime and the assignment of signals in the NMR spectra. Furthermore, the intensity of the split signals varies in the expected direction since the signals of free CHAPS gradually diminish and complexed CHAPS increase when the ratio  $[\beta\text{-CD}]/[\text{CHAPS}]$  increases.

The ROESY spectrum (Table 1) also supports the slow exchange rate condition since only cross-peaks involving signals assigned to complexed species are observed while signals assigned to free species are not involved. This general behavior is illustrated for a few protons in Figure 4a. It can be observed that there is not any cross-peak between the P18, P19, and P21 methyl groups of free CHAPS and any  $\beta$ -CD proton, but cross-peaks implying signals from complexed species are observed.

In addition to the P19/ $\beta$ -CD interactions, Figure 4b illustrates that the A and B rings of the steroid nucleus are also involved in the formation of a complex. The interactions of P2 and P6 with H3 and H5, and P4–H3 are quite evident (see Table 1).

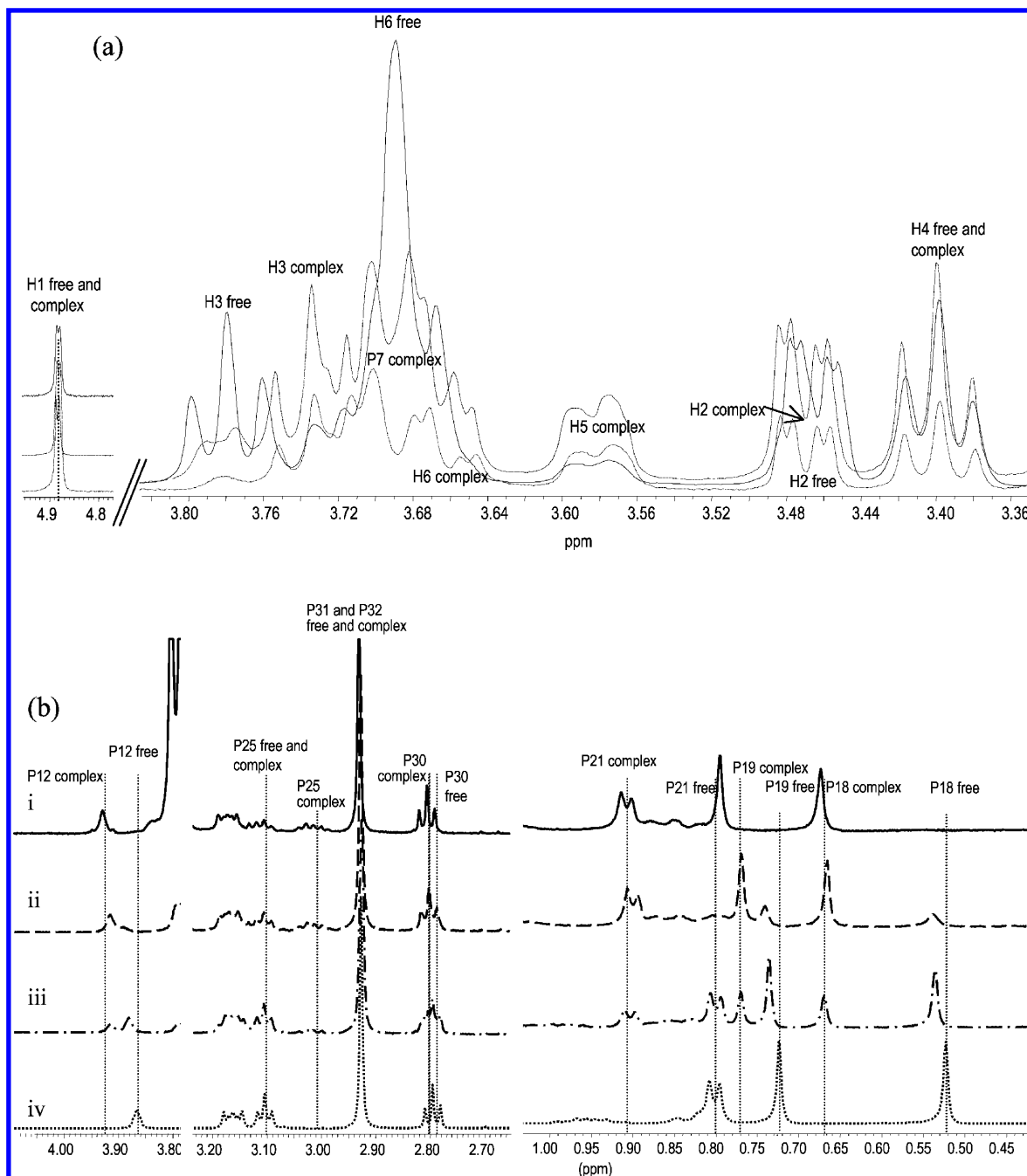


**Figure 3.** (a)  $^1\text{H}$  NMR spectra of the CHAPS/ $\beta$ -CD/ $\text{D}_2\text{O}$  system at the following concentrations: CHAPS 2 mM,  $\beta$ -CD 8 mM (solid line); CHAPS 5 mM,  $\beta$ -CD 5 mM (dashed line); CHAPS 8 mM,  $\beta$ -CD 2 mM (dot-dashed line). (b)  $^1\text{H}$  NMR spectra of the CHAPS/ $\beta$ -CD/ $\text{D}_2\text{O}$  system at the following concentrations: (i)  $\beta$ -CD 8 mM, CHAPS 2 mM; (ii)  $\beta$ -CD 5 mM, CHAPS 5 mM; (iii)  $\beta$ -CD 3 mM, CHAPS 7 mM; (iv)  $\beta$ -CD 1 mM, CHAPS 9 mM. It can be observed that the intensity of the signals of the free CHAPS gradually diminish with increasing  $\beta$ -CD concentration, while those of the complexed CHAPS increase.

In this table only irrefutable cross-peaks have been written, it is to say, some cross-peaks cannot be clearly distinguished since they are almost fully masked. This is the case of signals corresponding to the interactions P3–H3 and P1–H3 which are masked by the strong signals P28–H3 and P22–H3, respectively. We have also to remember the splitting of P5 and P6 which clearly suggest an interaction of  $\beta$ -CD with this region of CHAPS. (The region of the  $^1\text{H}$  NMR spectrum where the P2 signal appears is crowded. However, we exactly know the chemical shift for protons P2 thanks to their intramolecular ROESY interactions with P1, P4, and P9. The distances are around  $\text{P2}_{\text{axial}}\text{--P1}_{\text{equatorial}}$  2.3 Å,  $\text{P2}_{\text{axial}}\text{--P4}$  2.7 Å,  $\text{P2}_{\text{axial}}\text{--P9}$  2.3 Å, measured in a trihydroxy bile salt crystal. Once P2 are

located, the assignment of the  $\text{P2}_{\text{axial}}\text{--H5}$  cross-peak is straightforward.)

Protons of the side chain (for instance, P25) and C ring are also affected by the inclusion phenomena (see Table 1), and there is a remarkable absence of cross-peaks involving protons located at the D ring. Thus there are interactions of  $\beta$ -CD with CHAPS at two sites of the steroid nucleus, a first site being mainly the side chain, and A and B rings being the other one.

According to our previous experience with bile salts<sup>19,22</sup> and other steroids,<sup>18</sup> these facts suggest (i) the formation of a 1:2 complex, in which two  $\beta$ -CDs are simultaneously complexing the guest at the two sites, (ii) the formation of two different 1:1 complexes, or (iii) the existence of all these complexes.



**TABLE 1: ROESY Intermolecular Cross-Peaks Observed between CHAPS Protons (named P) and  $\beta$ -CD or  $\gamma$ -CD Protons (named H)<sup>a</sup>**

location	atom	$\beta$ -CD/ CHAPS			$\gamma$ -CD/ CHAPS		
		H3	H5	H6	H3	H5	H6
A ring	P1						
	P2	m	m				
	P3						
	P4	m					
A/B ring	P5						
B ring	P6	m			m		
	P7	m	m				
B/C ring	P8						
	P9	s			m		
C ring	P11	m			s		
	P12	s	w		m	s	
	P14				s		
D ring	P15				s	s	m
	P16				s		
	P17				s	s	
	P18	s	w	w	s	s	s
C/D ring	P19	m			s	s	s
A/B ring side chain	P20	m			w		
	P21	s	s	s			
	P22	s		m	w		
	P23	w			m		
	P25	s			w		w
	P26	s			s		
	P27	s					m
	P28	s	m	m	m	d	
	P29	w		w	m		
	P30	s	m	m	s	s	s
	P31	s	s	s	s	s	s
	P32	s	s	s	s	s	s

<sup>a</sup> All concentrations (CHAPS,  $\beta$ -CD, or  $\gamma$ -CD) were 10 mM (w: weak, m: medium, s: strong).

Furthermore, the ROESY spectrum evidences a strong intramolecular interaction between the P21 methyl group and P12 of the C ring, but no other interactions have been observed between the side chain and the steroid body. This suggests that the side chain is unfolded inside the cyclodextrin cavity.<sup>19</sup> On the other hand, the two P25 protons appear as a single signal in free CHAPS and as a double signal when they are inside the  $\beta$ -CD cavity. This reflects that the conformational mobility of the side chain in the interior of the cavity is not fast enough to produce the equivalence of the two protons, i.e., the CHAPS side inside the  $\beta$ -CD is much more rigid than free in the bulk solution.

The intensity of a signal (peak area) in <sup>1</sup>H NMR spectra is proportional to the concentration of the species<sup>20</sup> and therefore it can be used for measuring concentrations, allowing the determination of equilibrium constants. Here not all of the signals are appropriate for this purpose as the following points have to be taken into consideration: (i) overlapping signals from pure species cannot be used as the data analysis is difficult; this is the case of P7 which appears at the same  $\delta$  value of H5 and H6. (ii) for the same reason, signals from complexes should not overlap with other ones from pure species; (iii) the split of signals should be as large as possible to reduce the experimental error. These requirements reduce the number of useful protons (or signals).

The careful analysis of all spectra recommends that only signals from protons P18, P19, P21, P25, P12, and H5 should be considered. Even so, Figure 3 evidences that all chosen signals partially overlap with adjacent ones. For this reason, it was necessary to evaluate the contribution of each *pure* signal

**TABLE 2: Relative Areas of the Indicated Protons of Guest (CHAPS) or Host ( $\beta$ -CD) in the Complex at Different Concentrations of Both Reactants**

[ $\beta$ -CD] <sub>0</sub> /mM	[CHAPS] <sub>0</sub> /mM	relative area/complex				
		H5 <sup>a</sup>	P12 <sup>b</sup>	P18 <sup>b</sup>	P19 <sup>c</sup>	P25 <sup>b</sup>
10	0	0				
9	1	0.109	1.234	2.699	2.848	0.797
8	2	0.205	1.116	2.727	2.872	0.851
7	3	0.343	1.110	2.643	2.775	0.850
6	4	0.536	0.987	2.435	2.547	0.771
5	5	0.710	0.892	2.063	2.121	0.680
4	6	0.792	0.570	1.412	1.427	0.474
3	7	0.886	0.393	0.978	0.980	0.303
2	8	0.868	0.212	0.567	0.510	0.198
1	9	0.906	0.077	0.273	0.193	0.115

<sup>a</sup> Data used to calculate  $K_{11}$ . <sup>b</sup> Data used to calculate  $K_{11}^Y$ . <sup>c</sup> Data used to calculate  $K_{11}^X$ .

to the total area under the experimental curve. For this purpose, each experimental signal (or group of signals) of a spectrum was resolved as a sum of single signals (corresponding to free and complexed species) described by Lorentzian functions. Calculations were performed by the Levenberg–Marquardt method implemented in a homemade program. The fitting parameters were the half-height width and maxima of the intensity- $\delta$  curve of each *pure* signal contributing to the total area of the experimental curve. Once the area of each single signal was known, the concentration of the species was obtained as follows.

The concentration of a species is given by eq 1

$$\text{area}_{N,i} = k \times [S_i] \quad (1)$$

where  $S_i$  can be a complex, free cyclodextrin, or free CHAPS,  $\text{area}_{N,i}$  is the signal area of the proton  $N$  in the species  $S_i$ , and  $k$  is a constant that depends on the experimental conditions of the NMR experiment (mainly accumulation of spectra), i.e., its value is only valid for a given spectrum. The constant  $k$  can be easily obtained from an unaffected signal by the inclusion phenomena. Figure 3b clearly shows that the P31–P32 signal (corresponding to the methyl groups bound to the charged nitrogen atom of the side chain) can be used for this purpose. Thus it can be written

$$\text{area}_{P31,P32} = k[\text{CHAPS}]_0 \quad (2)$$

where  $[\text{CHAPS}]_0$  is the total concentration of CHAPS in the solution. Therefore,

$$[S_i] = k'[\text{CHAPS}]_0 \frac{\text{area}_{N,i}}{\text{area}_{P31,P32}} \quad (3)$$

i.e.,  $[S_i]$  is proportional to the relative area of the nucleus  $N$  of the species  $i$  to the area of the P31–P32 signal. In eq 3, the proportional factor  $k'$  was introduced to take into account the number of equivalent protons of each integrated signal.

The stoichiometry of complexes is determined in a straightforward fashion by means of the continuous variation method (Job's plot).<sup>29</sup> Results of Table 2 (which resumes the experimental relative areas of the indicated protons in complexed species) were plotted according to this methodology. Figure 5 clearly shows that the maxima for all studied protons appear at  $X_{\beta\text{-CD}} = 0.5$ , indicating the formation of complexes with a 1:1 stoichiometry. This stoichiometry is supported by the

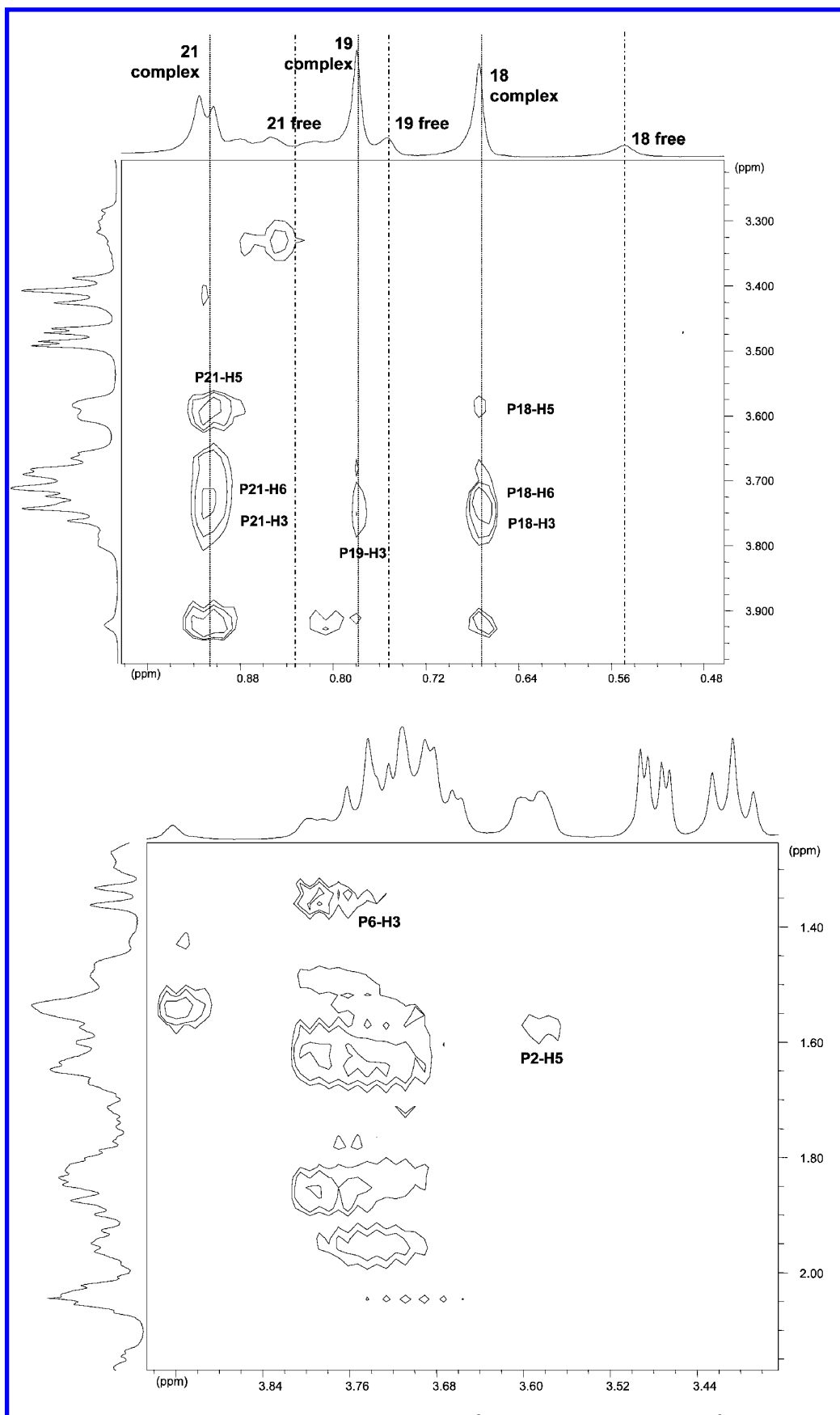


**Figure 4.** Significant cross-peaks from the ROESY spectrum of the CHAPS/ $\beta$ -CD system (CHAPS 10 mM,  $\beta$ -CD 10 mM).

analysis of the chemical shifts of protons of both the guest (Figures 5a and 5b) and the host (Figure 5c). As the central region of the steroid is too big to cross through the cavity of

the  $\beta$ -CD, these plots and the ROESY experiments suggest that two different 1:1 complexes ( $C_{11}^X$  and  $C_{11}^Y$ ) exist in solution. (Even for the system  $\gamma$ -CD/bile salts, there are no

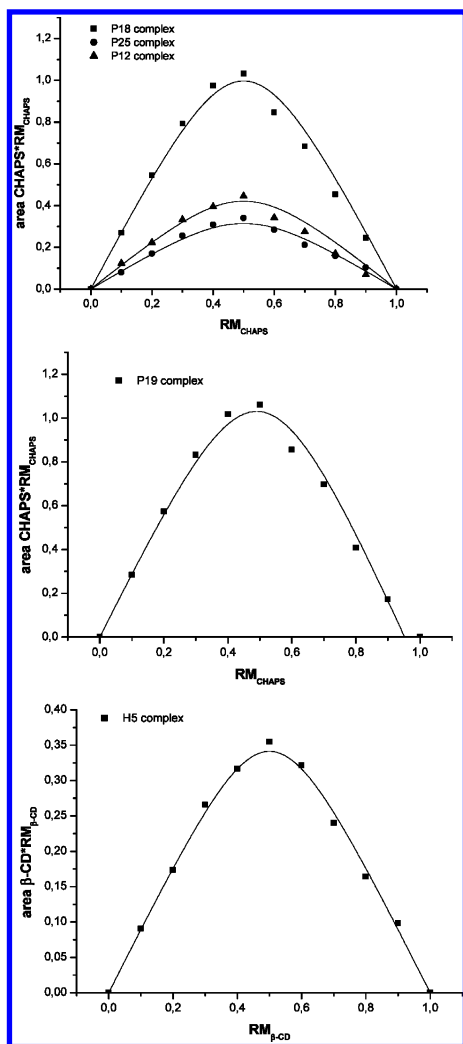
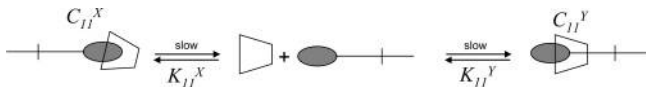
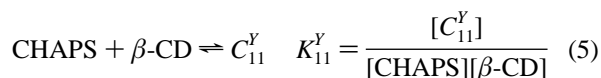
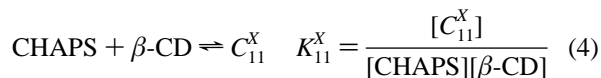


**Figure 5.** Job's plot of the indicated protons for the CHAPS/ $\beta$ -CD system in  $D_2O$ .

#### SCHEME 1



interactions between the protons of the A ring with any proton of the  $\gamma$ -CD.<sup>22</sup> This is also the case for  $\gamma$ -CD/CHAPS as we show below.) Their equilibrium reactions are given in eqs 4 and 5 (see also Scheme 1).



With the association constants  $K_{11}^X$  and  $K_{11}^Y$  and mass balances ( $[\text{CD}]_0$  and  $[\text{CHAPS}]_0$  being the total concentrations of  $\beta$ -CD and CHAPS in the solution and  $[\text{CD}]$  and  $[\text{CHAPS}]$  being the concentration of the free species of cyclodextrin and CHAPS, respectively)

$$\begin{aligned} [\text{CD}]_0 &= [\text{CD}] + [C_{11}^X] + [C_{11}^Y] \\ [\text{CHAPS}]_0 &= [\text{CHAPS}] + [C_{11}^X] + [C_{11}^Y] \end{aligned} \quad (6)$$

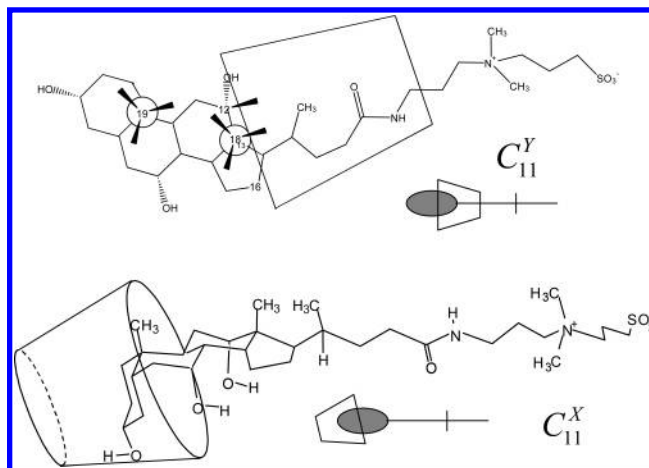


**Figure 6.** Schematic representation of the two isomeric 1:1 CHAPS/ $\beta$ -CD complexes deduced from ROESY and  $^{13}\text{C}$  NMR experiments. It must be noticed that in the  $C_{11}^Y$  complex, the orientation of the plane formed by the H3 protons of  $\beta$ -CD is parallel to the plane formed by C11, C13, C16, and C18 of CHAPS.

the following equations are obtained:

$$\begin{aligned} [C_{11}^X] &= \frac{K_{11}^X[\beta\text{-CD}][\text{CHAPS}]_0}{1 + (K_{11}^X + K_{11}^Y)[\beta\text{-CD}]} \\ [C_{11}^Y] &= \frac{K_{11}^Y[\beta\text{-CD}][\text{CHAPS}]_0}{1 + (K_{11}^X + K_{11}^Y)[\beta\text{-CD}]} \end{aligned} \quad (7)$$

$$[\beta\text{-CD}]^2 + \left( [\text{CHAPS}]_0 - [\beta\text{-CD}]_0 + \frac{1}{K_{11}^X + K_{11}^Y} \right) [\beta\text{-CD}] - \frac{[\beta\text{-CD}]_0}{K_{11}^X + K_{11}^Y} = 0 \quad (8)$$

Obviously, the sum of eqs 7 gives the total concentration of the  $\beta$ -CD involved in the formation of complexes

$$[C_{11}] = [C_{11}^X] + [C_{11}^Y] = \frac{(K_{11}^X + K_{11}^Y)[\beta\text{-CD}][\text{CHAPS}]_0}{1 + (K_{11}^X + K_{11}^Y)[\beta\text{-CD}]} \quad (9)$$

$[C_{11}]$  being the concentration of a 1:1 pseudo-complex with a pseudo (or macroscopic) equilibrium constant given by eqs 10 and 11

$$K_{11} = K_{11}^X + K_{11}^Y \quad (10)$$

$$[\text{CHAPS}][\beta\text{-CD}] \rightleftharpoons C_{11} \quad K_{11} = \frac{[C_{11}]}{[\text{CHAPS}][\beta\text{-CD}]} \quad (11)$$

The concentration of each individual complex can be determined from eq 3 by choosing the appropriate signals in the spectrum. ROESY results suggest the use of the signals from P12, P18, and P25 protons for the complex at the first site,  $C_{11}^Y$ , and the signal due to P19 protons for the complex at the second site,  $C_{11}^X$  (Figure 6). As we have already noticed, there is a strong intramolecular interaction between P21 and P12 since they are close to each other in the space. This proximity can also be observed in some bile salt crystals and suggests that those protons must be affected by the same cyclodextrin unit. To simultaneously affect both P21 and P12 protons, the orientation of the plane formed by the H3 protons of  $\beta$ -CD must be parallel to the plane formed by C11, C13, C16, and C18 of

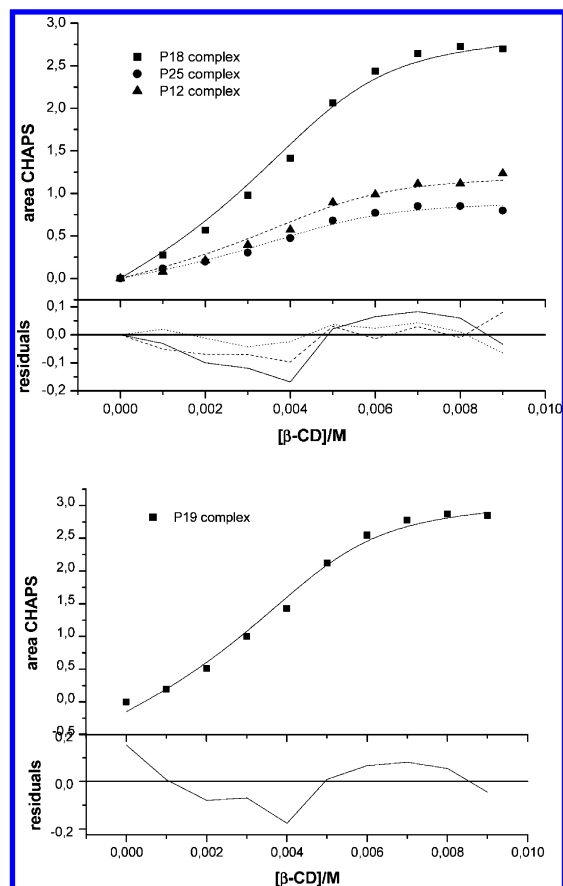


**Figure 7.** Plots of the areas measured for the indicated protons of the guest for the CHAPS/ $\beta$ -CD system in  $D_2O$  vs. the concentration of  $\beta$ -CD. Solid lines are the result of the nonlinear fitting, and the residuals are also plotted.

CHAPS. This orientation explains the absence of interactions between H3 and other protons of the D ring. This can easily be visualized with the help of molecular models.

By solving eq 8, and substitution of  $[\beta\text{-CD}]$  in eqs 7, the two microscopic equilibrium constants,  $K_{11}^X$  and  $K_{11}^Y$ , can be independently determined by fitting the experimental results, the equilibrium constants being the optimization parameters. The values obtained are  $(1.39 \pm 0.39) \times 10^3 \text{ M}^{-1}$  for  $K_{11}^X$  and  $(1.34 \pm 0.59) \times 10^3 \text{ M}^{-1}$  for  $K_{11}^Y$ . Figure 7 evidences the quality of the fittings.

Under slow exchange conditions, the number of split signals for a given nucleus should be equal to the number of species in solution. Although three signals are expected in theory for each nucleus of CHAPS corresponding to the two complexes and the free species, each complex contains only part of CHAPS within the cyclodextrin torus. The excluded portion of CHAPS in each complex would be expected to exhibit the same chemical shifts as free CHAPS. Thus for most protons and carbons, only two signals are expected. Protons from near the edge of the binding portion would be expected to exhibit three signals, but this does not seem to be the case here. Furthermore, a split in three signals can be expected for the cyclodextrin nuclei, although if the electronic environment inside the  $\beta$ -CD in the two complexes is not very different, these signals will appear fully overlapped. On the other hand the overlapping and width of proton signals in  $^1\text{H}$  NMR spectra (see for instance H5 signal of the complexed species in Figure 3) avoids the detection (without ambiguity) of the actual number of signals resulting from the split. Thus the area under H5 ( $\delta$  3.58 ppm) will be proportional to the sum of concentrations of the two complexes

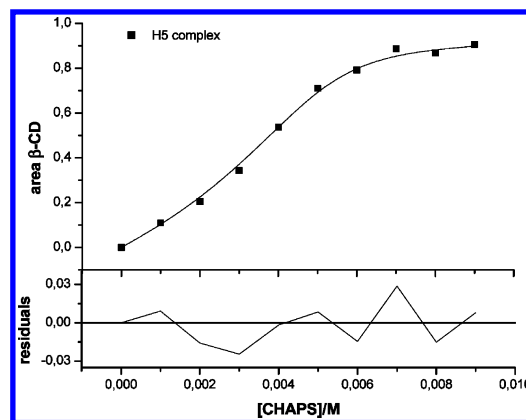


**Figure 8.** Plot of the area measured for H5 of the  $\beta$ -CD vs. the concentration of CHAPS. Solid line is the result of the nonlinear fitting, and the residuals are also plotted.

formed. This is equivalent to accept that, from the point of view of the  $\beta$ -CD, only one pseudo-complex,  $C_{11}$ , has been obtained. Therefore the analysis of the relative area data for H5 (Table 2) will lead to the determination of the macroscopic equilibrium constant  $K_{11}$ . For this purpose the sum  $K_{11}^X + K_{11}^Y$  is substituted by  $K_{11}$  in eqs 8 and 9. From the optimization process a value of  $K_{11} = (2.17 \pm 0.60) \times 10^3 \text{ M}^{-1}$  is obtained (Figure 8 represents the experimental values, the fitting curve, and the residuals). Although errors in the equilibrium constant values are high (a common fact in the determination of equilibrium constants from NMR experiments),<sup>18</sup> the agreement between the values determined for  $K_{11}$  and  $K_{11}^X + K_{11}^Y$  is really good. The ratio  $K_{11}^X/K_{11}$  can be used to measure the asymmetry of the ditopicity of the guest against a given host. Obviously, in this case the ratio is almost equal to 0.5, and therefore, although the chemical structure at both sides of the CHAPS is different, the  $\beta$ -CD does not distinguish between them. This is in agreement with the low specific character of cyclodextrins in complexing many organic guests.

The value of  $K_{11}^Y$  is comparable with values for the equilibrium constant of the complex formation between trihydroxy bile salts and  $\beta$ -CD, for which values ranging from  $7.5 \times 10^3 \text{ M}^{-1}$  for sodium cholate to  $1.8 \times 10^3 \text{ M}^{-1}$  for sodium taurocholate have been published.<sup>22</sup> Thus, all the systems have  $\Delta G^\circ$  values in a very narrow range.

On the other hand, as the two sites of the CHAPS can form complexes with  $\beta$ -CD, the formation of a 1:2 complex could be expected. We have analyzed this possibility by introducing the corresponding equilibria and the associated constants. The mathematical analysis was carried out through the introduction of the interaction parameter from Connors et al.,<sup>11,12</sup> which measures the cooperativity for the interaction between the two sites in the formation of a 1:2 complex. However, the convergence in the analysis of data was achieved only when very low values (lower than  $10^{-4}$ ) of that parameter were used. Therefore, within experimental error, the model of the formation of two 1:1 isomeric complexes is essentially correct.

The fast exchange condition<sup>17</sup> was observed for bile salt systems, while in this case the system obeys the slow exchange rate condition. As we have commented, all these systems have  $\Delta G^\circ$  values in a very narrow range, independently of the exchange rate condition. This means that the activation parameters (and therefore the kinetic constants) for the formation and decomposition of complexes vary in the same amount for both bile salts/ $\beta$ -CD and CHAPS/ $\beta$ -CD systems, being higher (lower kinetic constants) for the last one. Since Table 2 evidences that there are interactions between the cyclodextrin protons and C



and D rings of the steroid nucleus, the entire side chain (which also shows such interactions) has traveled all along the cyclodextrin cavity. Therefore, the lower kinetic constants for the formation and decomposition of the  $C_{11}^Y$  complex can be understood as a barrier penetration problem for the side chain to cross through the cyclodextrin cavity since the methyl groups P31 and P32 are bulky enough to force a large distortion of the  $\beta$ -CD during the penetration. Furthermore, they are linked to a charged nitrogen atom which, being hydrated, must probably lose the water molecules (leaving a naked charged nitrogen) before entering inside the cavity. Obviously these two facts increase the thermodynamic activation parameters in both directions. A similar example has been given by Yonemura et al.<sup>31</sup> when studying the interaction between cyclodextrins and carbazole–viologen linked compounds.

The protons of the side chain do not interact with those of the steroid rings, suggesting that it is most unfolded outside the cyclodextrin cavity forming a rotaxane-type structure (Figure 6). Lyon et al.<sup>32</sup> have investigated the kinetics and mechanism of the formation and dissociation of a series of [2]pseudorotaxanes, consisting of  $\alpha$ -CD as the cyclic component and several tetraalkylammonium dications as the threads in aqueous solution. It is interesting to notice that they observe a decrease of the enthalpies and entropies of activation for the formation and dissociation of the [2]pseudorotaxanes with an increase in the size and hydrophobicity of the end groups. According to these authors, this fact suggests a reduced role of desolvation of the quaternized atoms in the threading or dethreading processes.

Furthermore, the inclusion of the side chain of CHAPS inside the  $\beta$ -CD confers it a rigidity which allows to differentiate the two protons of the same methylene group in the NMR spectrum. This is not possible when CHAPS is free.

Much less clear is the origin of the energy barrier for the complexation of the wide end of the steroid nucleus leading to a slow exchange regime, since for the complexation of dihydroxy bile salts the fast exchange regime was observed.<sup>22</sup> Furthermore, the steroid nuclei (including hydroxy substituents) of trihydroxy bile salts and CHAPS have exactly the same structure, the only difference being the side chain, but the complexation by the wide end of trihydroxy bile salts was not observed. Therefore these two differences can be related to the side chain. It is known that the side chain has an extraordinary influence on the behavior of bile salts, at least when they are arranged as in solid state.<sup>33</sup> The influence is also prominent in their biological properties since conjugated (with glycine or taurine) bile acids are more soluble at the pH prevailing in the small intestine, are resistant to precipitation by  $Ca^{2+}$  ions, and are membrane-impermeable. If exists, the possible role of the side chain by this side of the steroid nucleus is still unknown. On the other hand, preliminary studies on the complexation of sodium ursodeoxycholate by  $\beta$ -CD evidence a slow exchange regime (NMR time scale) for its two complexing sites (analogous to those of CHAPS). The structural differences between deoxycholate, a dihydroxy bile salt (which forms a 1:2 complex with  $\beta$ -CD), for which fast exchange regime was observed, and ursodeoxycholate are located in the B ring and concern the position and spatial orientation of the hydroxy group while the C and D rings and the side chain are identical in both compounds. Thus it seems that the slow rate regimen *simultaneously* affects both sites of the guest.

The formation of a rotaxane type structure by the side chain of CHAPS, with a transition state corresponding to the cross of the methyl groups P31 and P32 through the  $\beta$ -CD cavity, suggests that a larger cyclodextrin cavity will have lower

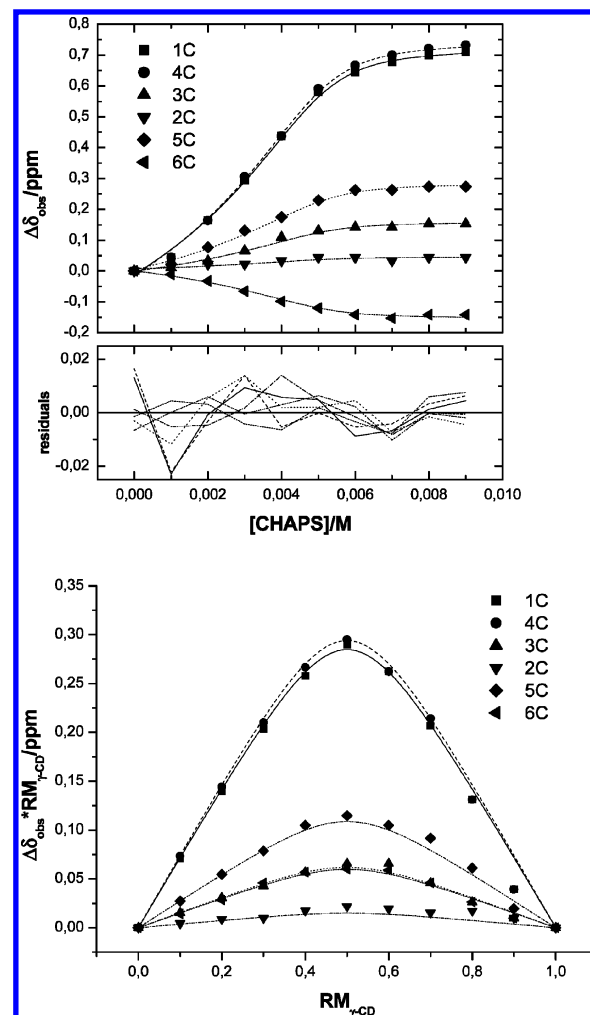


**Figure 9.** Plot of the chemical shift displacements,  $\Delta\delta_{\text{obs}}$ , of different  $\gamma$ -CD carbons vs. the concentration of  $\gamma$ -CD and the corresponding Job's plots. Solid lines are the result of the nonlinear fitting. The residuals are also plotted.  $[\text{CHAPS}] + [\gamma\text{-CD}] = 10 \text{ mM}$ .  $\text{RM}_{\gamma\text{-CD}}$  is the molar ratio for  $\gamma$ -CD, i.e.,  $[\gamma\text{-CD}]/([\gamma\text{-CD}] + [\text{CHAPS}])$ .

**TABLE 3: Equilibrium Constant and Maxima Chemical Shift Displacements for the 1:1 Complex Formed by CHAPS and  $\gamma$ -CD Obtained from  $^{13}\text{C}$  NMR Measurements at 25 °C**

$10^{-3}K_{11}/\text{M}^{-1}$	carbon atom	CHAPS $\Delta\delta_{\text{max}}/\text{ppm}$
$3.6 \pm 0.4$	C1	$0.7440 \pm 0.0095$
	C2	$0.0389 \pm 0.0076$
	C3	$0.1616 \pm 0.0077$
	C4	$0.7683 \pm 0.0096$
	C5	$0.2842 \pm 0.0079$
	C6	$-0.1564 \pm 0.0077$

activation energies and that the fast exchange limit could be obeyed. Therefore, complexation studies between CHAPS and  $\gamma$ -CD (diameter 8.5 Å) were undertaken. Figure 9 shows the chemical shift displacements of carbon atoms of  $\gamma$ -CD (determined from  $^{13}\text{C}$  NMR experiments) with increasing CHAPS concentration, and the corresponding Job's plots. The figure confirms the fast exchange and the formation of a complex with a 1:1 stoichiometry. Data analyses under fast exchange conditions have been widely discussed elsewhere.<sup>18,22</sup> The obtained results for the equilibrium constant and maximum chemical shift displacements,  $\Delta\delta_{\text{max}}$ , are summarized in Table 3. The obtained values for  $K_{11}$  and  $\Delta\delta_{\text{max}}$  (for all carbon atoms) are very similar to those for bile salts,<sup>22</sup> suggesting that the more stable structure of the complex has the rings C and D completely inside the

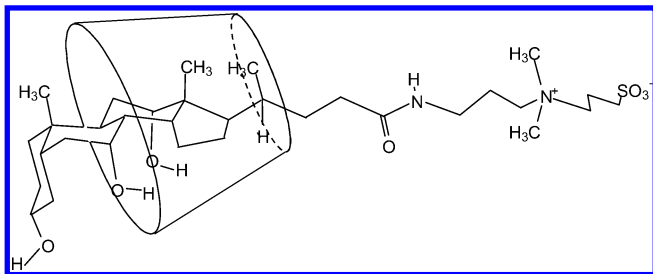


**Figure 10.** Schematic representation of the 1:1 CHAPS/ $\gamma$ -CD complex deduced from ROESY and  $^{13}\text{C}$  NMR experiments.

cyclodextrin cavity reaching the P19 methyl group. This is confirmed by the ROESY spectrum (Table 1), which is also very similar to those observed for trihydroxy bile salts/ $\gamma$ -CD systems. There are strong interactions between the P31 and P32 methyl groups and  $\gamma$ -CD protons, and the interactions extend all over the side chain. As the strongest interactions of the C and D rings of the steroid nucleus are with H3, it may be concluded that the side chain enters the  $\gamma$ -CD through its secondary hydroxyl rim. The rotaxane structure for this complex is shown in Figure 10.

**Acknowledgment.** The authors thank the Ministerio de Ciencia y Tecnología (Project MAT2001-2911) for financial support. R.M.B. and V.H.S. thank CAPES (Brazil) and AECI (Beca Mutis)/University of Costa Rica, respectively, for research scholarships. The authors thank to Professor Bruce Grindley for helpful discussions.

## References and Notes

- (1) Ladbury, J. E.; Chowdhry, B. Z. *Biocalorimetry. Applications of Calorimetry in the Biological Sciences*; Wiley & Sons: Chichester, 1998.
- (2) Gopal, B.; Swaminathan, C. P.; Bhattacharya, S.; Bhattacharya, A.; Murthy, M. R. N.; Suroliya, A. *Biochemistry* **1997**, *36*, 10910.
- (3) Huang, S. T.; Choi, W. E.; Bloom, C.; Leuenberger, M.; Dunn, M. F. *Biochemistry* **1997**, *36*, 9878.
- (4) Colquhoun, D.; Ogden, D. C. *J. Physiol.* **1988**, *395*, 131.
- (5) Bornhorst, J. A.; Falke, J. J. *Biochemistry* **2000**, *39*, 9486.
- (6) Grant, G. A.; Xu, X. L.; Hu, Z.; Purvis, A. R. *Biochemistry* **1999**, *38*, 16548.
- (7) Park, H.; Bradrick, T. D.; Howell, E. E. *Protein Eng.* **1997**, *10*, 1415.
- (8) Thoenges, D.; Schoner, W. *J. Biol. Chem.* **1997**, *272*, 16315.
- (9) Thoenges, D.; Amler, E.; Eckert, T.; Schoner, W. *J. Biol. Chem.* **1999**, *274*, 1971.
- (10) Roberts, G.; Beauge, L. *Eur. J. Biochem.* **1997**, *246*, 228.
- (11) Connors, K. A.; Pendergast, D. D. *J. Am. Chem. Soc.* **1984**, *106*, 7607.
- (12) Connors, K. A.; Paulson, A.; Toledo-Velasquez, D. *J. Org. Chem.* **1988**, *53*, 2023.
- (13) Sur, S. K.; Bryant, R. G. *J. Phys. Chem.* **1995**, *99*, 4900.
- (14) Alvarez-Parrilla, E.; Al-Soufi, W.; Ramos Cabrer, P.; Novo, M.; Vázquez Tato, J. *J. Phys. Chem. B* **2001**, *105*, 5994.
- (15) Maki, H.; Nariai, H. *Phosphorus Lett.* **2001**, *40*, 33.
- (16) Hirose, K. *J. Inclusion Phenom. Macrocyclic Chem.* **2001**, *39*, 193.
- (17) Connors, K. A. *Binding Constants: the Measurement of Molecular Complex Stability*; Wiley: New York, 1987.
- (18) Al-Soufi, W.; Ramos Cabrer, P.; Jover, A.; Budal, R. M.; Vázquez Tato, J. *Steroids* **2003**, *68*, 43.
- (19) Ramos Cabrer, P.; Alvarez-Parrilla, E.; Mejjide, F.; Seijas, J. A.; Rodríguez Núñez, E.; Vázquez Tato, J. *Langmuir* **1999**, *15*, 5489.
- (20) Cameron, K. S.; Fletcher, D.; Fielding, L. *Magn. Res. Chem.* **2002**, *40*, 251.
- (21) Kempfle, M. A.; Mueller, R. F.; Palluk, R.; Winkler, H. A. *Biochim. Biophys. Acta* **1987**, *923*, 83.
- (22) Ramos Cabrer, P.; Alvarez-Parrilla, E.; Al-Soufi, W.; Mejjide, F.; Rodríguez Núñez, E.; Vázquez Tato, J. *Supramol. Chem.* **2003**, *15*, 33.
- (23) Funasaki, N.; Hada, S.; Neya, S. *J. Phys. Chem.* **1991**, *95*, 1846.
- (24) Funasaki, N.; Ueshiba, R.; Hada, S.; Neya, S. *J. Chem. Soc., Faraday Trans.* **1993**, *89*, 4355.
- (25) Hjelmeland, L. M. *Proc. Natl. Acad. Sci. U.S.A.* **1980**, *77*, 6368.
- (26) Stark, R. E.; Leff, P. D.; Milheim, S. G.; Kropf, A. *J. Phys. Chem.* **1984**, *88*, 6063.
- (27) González-Gaitano, G.; Compostizo, A.; Sánchez-Martin, L.; Tardajos, G. *Langmuir* **1997**, *13*, 2235.
- (28) Ramos Cabrer, P. Doctoral Thesis, Universidad de Santiago de Compostela, Spain, 2000.
- (29) Gil, V. M. S.; Oliveira, N. C. *J. Chem. Educ.* **1990**, *67*, 473.
- (30) Szejtli, J. *Cyclodextrin Technology*; Kluwer Academic Publishers: Dordrecht, The Netherlands, 1988.
- (31) Yonemura, H.; Kasahara, M.; Saito, H.; Nakamura, H.; Matsuo, T. *J. Phys. Chem.* **1992**, *96*, 5765.
- (32) Lyon, A. P.; Banton, N. J.; Macartney, D. H. *Can. J. Chem.* **1998**, *76*, 843.
- (33) Kato, K.; Sugahara, M.; Tohnai, N.; Sada, K.; Miyata, M. *Cryst. Growth Design* **2004**, *4*, 263.
- (34) Bender, M. L. *Cyclodextrins as Enzyme Models in Solution Behavior of Surfactants*; Mittal, K. L., Fendler, E. J., Eds.; Plenum Press: New York, 1982; Vol. 2, p 1171.
- (35) Bender, M. L.; Komiyama, M. *Cyclodextrin Chemistry*; Springer-Verlag: Berlin, 1978.
- (36) Breslow, R. *Recl. Trav. Chim. Pays-Bas* **1994**, *113*, 493.
- (37) Breslow, R. *Pure Appl. Chem.* **1990**, *62*, 1859.
- (38) Marzona, M.; Carpignano, R.; Quagliotto, P. *Ann. Chim.* **1992**, *82*, 517.
- (39) Albers, E.; Muller, B. W. *J. Pharm. Sci.* **1992**, *81*, 756.
- (40) Breslow, R.; Zhang, B. *J. Am. Chem. Soc.* **1996**, *118*, 8495.
- (41) Asanuma, H.; Kakazu, M.; Shibata, M.; Hishida, T.; Komiyama, M. *Chem. Commun.* **1997**, 1971.
- (42) Ravichandran, R.; Divakar, S. *J. Inclusion Phenom. Mol. Recognit. Chem.* **1998**, *30*, 253.
- (43) Taneva, S.; Ariga, K.; Okahata, Y.; Tagaki, W. *Langmuir* **1989**, *5*, 111.
- (44) Karuppiyah, N.; Kaufman, P. B.; Kapustka, S. A.; Sharma, A. *Microchem. J.* **1993**, *47*, 325.
- (45) Frijlink, H. W.; Eissens, A. C.; Hefting, N. R.; Poelstra, K.; Lerk, C. F.; Meijer, D. K. F. *Pharm. Res.* **1991**, *8*, 9.
- (46) Claudy, P.; Letoffe, J. M.; Germain, P.; Bastide, J. P.; Bayol, A.; Blasquez, S.; Rao, R. C.; González, B. *J. Thermal. Anal.* **1991**, *37*, 2497.
- (47) Sreenivasan, K. *J. Appl. Polym. Sci.* **1998**, *68*, 1857.
- (48) Tan, X.; Lindenbaum, S. *Int. J. Pharm.* **1991**, *74*, 127.
- (49) Alvarez Parrilla, E.; Ramos Cabrer, P.; Singh, A. P.; Al-Soufi, W.; Mejjide, F.; Rodríguez Núñez, E.; Vázquez Tato, J. *Supramol. Chem.* **2002**, *14*, 397.
- (50) Breslow, R.; Halfon, S.; Zhang, B. *Tetrahedron* **1995**, *51*, 377.
- (51) Zhang, B.; Breslow, R. *J. Am. Chem. Soc.* **1993**, *115*, 9353.
- (52) Breslow, R.; Belvedere, S.; Gershell, L.; Leung, D. *Pure Appl. Chem.* **2000**, *72*, 333.
- (53) Breslow, R.; Greenspoon, N.; Guo, T.; Zarzycki, R. *J. Am. Chem. Soc.* **1989**, *111*, 8296.
- (54) Breslow, R.; Chung, S. *J. Am. Chem. Soc.* **1990**, *112*, 9659.
- (55) Breslow, R. *Supramol. Chem.* **1993**, *1*, 111.
- (56) Breslow, R. *Isr. J. Chem.* **1992**, *32*, 23.
- (57) Breslow, R.; Zhang, X.; Xu, R.; Maletic, M.; Merger, R. *J. Am. Chem. Soc.* **1996**, *118*, 11678.
- (58) Alvarez Parrilla, E.; Ramos Cabrer, P.; Al-Soufi, W.; Mejjide, F.; Rodríguez Núñez, E.; Vázquez Tato, J. *Angew. Chem., Int. Ed.* **2000**, *39*, 2856.
- (59) Harada, A.; Kawaguchi, O.; Hoshino, T. *J. Inclusion Phenom. Macrocyclic Chem.* **2001**, *41*, 115.